Engineering in Life Sciences

*Eng. Life Sci.* **2018**, *18*, 298–307 www.els-journal.com

**Javad Mohammadnejad**[1]*
**Fatemeh Yazdian**[1]
**Meisam Omidi**[2]
**Arash Darzian Rostami**[1]
**Behnam Rasekh**[3]
**Atena Fathinia**[1]

[1] Department of Life Science Engineering, Faculty of New Sciences and Technologies, University of Tehran, Tehran, Iran

[2] Department of Tissue Engineering and Regenerative Medicine, School of Advanced Technologies in Medicine, Shahid Beheshti University of Medical sciences, Tehran, Iran

[3] Microbiology and Biotechnology Research Group, Research Institute of Petroleum Industry, Tehran, Iran

Research Article

# Graphene oxide/silver nanohybrid: Optimization, antibacterial activity and its impregnation on bacterial cellulose as a potential wound dressing based on GO-Ag nanocomposite-coated BC

Recently, bacterial cellulose (BC) based wound dressing have raised significant interests in medical fields. However, to our best knowledge, it is apparent that the BC itself has no antibacterial activity. In this study, we optimized graphene oxide-silver (GO-Ag) nanohybrid synthesis using Response Surface Methodology and impregnate it to BC and carefully investigate their antibacterial activities against both the Gram-negative bacteria *Escherichia coli* and the Gram-positive bacteria *Staphylococcus aureus*. We discover that, compared to silver nanoparticles, GO-Ag nanohybrid with an optimal GO suspension's pH and $\frac{[GO]}{[AgNO_3]}$ ratio is much more effective and shows synergistically enhanced, strong antibacterial activities at rather low dose. The GO-Ag nanohybrid is more toxic to *E. coli* than that to *S. aureus*. The antibacterial and mechanical properties of BC/GO-Ag composite are further investigated.

**Keywords:** Antibacterial effects / Bacterial cellulose / Graphene oxide/Silver nanohybrid / Nanocomposite / Wound dressing

*Received:* August 8, 2017; *revised:* November 29, 2017; *accepted:* January 31, 2018

**DOI:** 10.1002/elsc.201700138

## 1 Introduction

Advanced approaches to wound healing have attracted much attention in the last decades due to the use of novel types of dressing that takes an active part in wound protection. The use of bacterial cellulose (BC) is attractive for advanced wound management because of favorable characteristics of BC such as high purity, biocompatibility, structural crystallinity, oxygen permeability, high water absorption capacity and extremely hydrophilic surface, high tensile strength, homologous structure, excellent biodegradability, biological properties and non-toxicity. However, BC itself does not have antibacterial activity and this may reduce its effectiveness as a treatment for wounds [1].

The deficiencies mentioned above limit the application of BC in different fields; thus, there is a need for a synthesis of its composites. Owing to its structural features, BC has shown tremendous potential as a matrix in the synthesis of various composite materials. BC composites have been formed using a broad range of materials ranging from nanoparticles to polymers, many of which have been synthesized to enhancing antibacterial properties of BC [2, 3].

In general, inorganic nanomaterials play an important role in antibacterial applications due to their large surface area and the properties imparted by their particle shapes [4]. Metal and metal oxide nanoparticles, well known for their highly potent antibacterial effect, include silver (Ag), titanium oxide ($TiO_2$), copper oxide (CuO), and zinc oxide (ZnO). Like other polymeric materials, BC can be used to make composites with metals and metallic oxides through a variety of synthetic approaches [5, 6].

A wide variety of BC composites has also been explored as potential wound dressing materials. Several studies have attempted to found and investigate matrices impregnated with antibacterial active nanoparticles [7]. Numerous studies have shown that BC/Ag composite has antibacterial activity against both Gram-positive and Gram-negative bacteria [8–10]. Katepetch et al. (2013) found BC composite with ZnO

**Correspondence**: Dr. Meisam Omidi (maysam.omidi@gmail.com), Department of Tissue Engineering and Regenerative Medicine, School of Advanced Technologies in Medicine, Shahid Beheshti University of Medical sciences, Tehran, Iran

**Abbreviations: BC**, Bacterial cellulose; **GO**, Graphene oxide; **NPs**, Nanoparticles

*Additional correspondence: Dr. Javad Mohamadnejad (mohamadnejad@ut.ac.ir), Department of Life Science Engineering, Faculty of New Sciences and Technologies, University of Tehran, Tehran, Iran

nanoparticles has antibacterial activity against *E. coli* and *S. aureus*. The composite was fabricated by ultrasonic assisted in situ precipitation of zinc oxide onto the BC surface, resulting in the formation of nanocrystalline particles without affecting the 3D structure of the BC substrate [11]. Recent studies report the effectiveness of BC-based antibacterial dressings with impregnated $TiO_2$ nanoparticles against some strains of Gram-positive and Gram-negative bacteria as well as against yeast colonies. In addition to antibacterial properties, the RBC-$TiO_2$ nanocomposites showed impressive cell adhesion and proliferation capabilities with animal fibroblast cells without showing any toxic effects [12]. In another major study, Shao et al. (2015) found that BC composites with graphene oxide (GO) proved excellent antibacterial activity against *E. coli* and *S. aureus* [13].

Graphene oxide, a two-dimensional carbon material, has attracted a great deal of attention [14]. Apart from the layered structure with a large theoretical specific surface area, GO nanosheets bear abundant oxygen-containing surface groups, such as hydroxyl, epoxide, carbonyl and carboxyl groups [15]. The presence of such groups not only allows the GO sheets to be well dispersed in water to yield a colloidally stable suspension, but also offers potential application as nanoscale substrates for the fabrication of flexible GO based composite materials. For instance, GO has been employed as a support to anchor gold nanoparticles for catalytic applications [16]. Very recently, it has been reported that GO could inhibit the growth of *E. coli*. It has also been found that graphene and GO could damage the cell membrane by direct contact with the bacteria. This material has been used as a promising building block for preparing new composites. On the other hand, it is well-known that Ag-NPs possess antimicrobial activity and have been used as biocide agents in health, food and textile applications [17]. Accordingly, silver nanoparticles assembled on graphene oxide sheets have been exploited as novel antibacterial systems [18].

As mentioned above, some previous studies have reported the synthesis of GO-Ag nanocomposite and its antibacterial activity [18, 19]. To the best of our knowledge, no previous study has investigated effect of GO-Ag nanocomposite impregnation on BC. In this research, synthesis process of GO-Ag nanohybrid was optimized using Response Surface Methodology (RSM) and impregnate on BC and investigate their antibacterial activities and mechanical properties.

## 2 Materials and methods

*Gluconacetobacter xylinus* (strain PTCCC 1734), *Escherichia coli* and *Staphylococcus aureus* were purchased from Microbiological Resources Centre, Iranian Research Organization for Science and Technology. All materials were analytical grade and used without further purification.

### 2.1 Production of bacterial cellulose

The Hestrin and Schramm (HS) medium used for growing *G. xylinus* contains 20 g/L glucose, 5 g/L peptone, 5 g/L yeast extract, 1.15 g/L citric acid, 2.7 g/L $Na_2HPO_4$, 10 mL ethanol . HS medium was adjusted to pH 6.0 and autoclaved at 120°C for 20 min. After cooling, inoculum culture was prepared *by* transferring *G. xylinus* cell suspension stored at –70°C into 100 mL HS medium and statically cultivated at 30°C for 2 days, when the cell number reached to $3.2 \times 10^6$ cell per mL without any cellulose production. The statically grown culture was then inoculated into a HS media with 10 vol. % inoculation size and Incubated at 30°C for 7 days to produce bacterial cellulose. After incubation, bacterial cellulose pellicles produced on the surface of each liquid culture medium were harvested. The residue was then washed with abundant distilled water and purified by boiling them in 1.0% NaOH for 2 h, finally thoroughly washed in distilled water [20]. Then BC dewatered by the hot pressing device and dried at 40°C for 72 h.

### 2.2 Synthesis of nanoparticles

#### 2.2.1 Synthesis of graphene oxide (GO)

Graphene oxide was synthesized from graphite powder using modified Hummer's method. In brief, 1 g of graphite and 0.5 g of sodium nitrate were mixed together followed by the addition of 23 mL of concentrated sulphuric acid under constant stirring. After 1 h, 3 g of potassium permanganate ($KMnO_4$) was added gradually to the above solution while keeping the temperature less than 20°C to prevent overheating and explosion. The mixture was stirred at 35°C for 12 h and the resulting solution was diluted by adding 500 mL of water under vigorous stirring. To ensure the completion of reaction with $KMnO_4$, the suspension was further treated with 30% $H_2O_2$ solution (5 mL). The resulting mixture was washed with HCl and $H_2O$ respectively, followed by filtration and drying, graphene oxide sheets were thus obtained [21].

#### 2.2.2 Synthesis and optimization of graphene oxide-silver nanohybrid

For the preparation of GO-Ag nanohybrid, 10.0 mL of a homogeneous aqueous suspension containing 0.07 mg/mL of GO (with pHs: 5.4, 7.4, 9.4) was mixed with a defined mass of $AgNO_3$ (by fixing the amount of GO and varying the $AgNO_3$ weight, that provided $\frac{[GO]}{[AgNO_3]}$ ratio: 0.05, 0.15 and 0.25), and this volume was maintained under strong stirring (in dark room) for 90 min before adding the reducing agent. After this period, an amount of 40 mg of $NaBH_4$ for each mL of GO dispersion was added to the system. The reaction mixture was stirred for another 30 min. For isolation of nanohybrid, the suspension centrifuged at 4000 rpm for 10 min and then the supernatant was replaced with deionized water. This process repeated for two times [22]. In the aim of measuring amount of silver loaded on GO, Mohr's method was performed [23].

Optimization of GO-Ag nanohybrid formation parameters was performed by employing the response surface methodology (RSM). Based on the literature reviews, the significant independent variables that affecting GO-Ag nanohybrid formation are GO suspension's pH and $\frac{[GO]}{[AgNO_3]}$ ratio. The silver loaded on GO sheets was considered as the response. The central values (zero level) chosen for experimental design were pH = 7.4 for GO suspension and $\frac{[GO]}{[AgNO_3]}$ ratio = 0.15. Table 1 shows factors and levels used in the experimental design. Table 2 shows the designed experiments totally.

**Table 1.** Experimental range and levels of independent factors

| Independent factors | Levels | | |
|---|---|---|---|
| | −1 | 0 | +1 |
| **pH of GO suspension** | 5.4 | 7.4 | 9.4 |
| $\frac{[GO]}{[AgNO_3]}$ **ratio** | 0.05 | 0.15 | 0.25 |

**Table 2.** Design of experimental process based on RSM model for optimization of GO-Ag nanohybrid synthesis

| Number | Experimental design | |
|---|---|---|
| | pH | $\frac{[GO]}{[AgNO_3]}$ ratio |
| 1 | −1 | −1 |
| 2 | −1 | +1 |
| 3 | +1 | −1 |
| 4 | +1 | +1 |
| 5 | 0 | −1 |
| 6 | 0 | +1 |
| 7 | −1 | 0 |
| 8 | +1 | 0 |
| 9 | 0 | 0 |
| 10 | 0 | 0 |
| 11 | 0 | 0 |
| 12 | 0 | 0 |
| 13 | 0 | 0 |

### 2.3 Impregnation of GO-Ag nanohybrid into bacterial cellulose

According to information obtained from experimental design, optimized GO-Ag nanohybrid at optimal conditions of pH and $[\frac{[GO]}{[AgNO_3]}]$ ratio was synthesized. To impregnate GO-Ag nanohybrid into BC, the optimized GO-Ag nanohybrid solution sprayed on wet BC at room temperature. The resulting composite dewatered using the heat press machine significantly and then dried at 40°C for 3 days.

### 2.4 Tensile strength and elongation tests

The mechanical properties were evaluated by conducting tensile strength and elongation-at-break using a Texture Analyzer according to the ASTM standard method [24]. In these tests, pre-conditioned BC/GO-Ag composite cut into 1.0 cm (W) × 5.0 cm (L) strips and mounted between the grips of the machine with initial grip gap of 50 mm. Sample was uniaxially pulled until breaking at a cross-head speed of 2.0 mm/min. Each test trial consisted of five replicate measurements to obtain the average values. The results of tensile and elongation tests were expressed by MPa and percentage (%), respectively.

### 2.5 Characterization

The characterization of the prepared nanoparticles and composites were determined by UV absorption spectrum, Scanning Electron Microscope (SEM) and Transmission Electron Microscope (TEM) analysis. Further, characteristic was determined by X-ray Diffraction (XRD), Raman spectra, Fourier Transform Infrared Spectroscopy (FTIR) and Atomic force microscopy (AFM).

### 2.6 Evaluation of antibacterial activity

The antibacterial activity of GO and GO-Ag was evaluated by microdilution assays, as described by the Clinical and Laboratory Standards Institute (CLSI). To determine the minimal inhibitory concentration (MIC) *E. coli* and *S. aureus* were used as model microorganisms. The strains were cultivated in Mueller-Hinton broth incubated at 37°C for 24 h. The bacterial suspensions were diluted with Mueller-Hinton broth to $OD_{570} = 0.2$ and were distributed (100 $\mu$L) in a 96-well plate. Each well was exposed to different concentrations of GO and GO-Ag (from 1.0 to 100.0 $\mu$g/mL). The plates were incubated at 37°C, and the bacterial growth was observed after 18 h. The test was repeated three times. The MIC was considered as the lowest nanomaterial concentration where no bacterial growth was visualized.

To investigate the antibacterial properties of BC/GO-Ag composite, a similar procedure was followed and each well was exposed to the bacteria suspension cultured on equal parts of pure BC and BC/GO-Ag. After incubation for 20 h at 37°C, the MIC was determined by visual examinations on the basis of the lowest concentration of sample solution in cells with no bacterial growth [19].

## 3 Results and discussion

### 3.1 Characterization

#### *3.1.1 Bacterial cellulose*

The results obtained from the SEM and FTIR analysis of BC produced by *G. xylinus* are shown in Figs. 1 and 2, respectively.

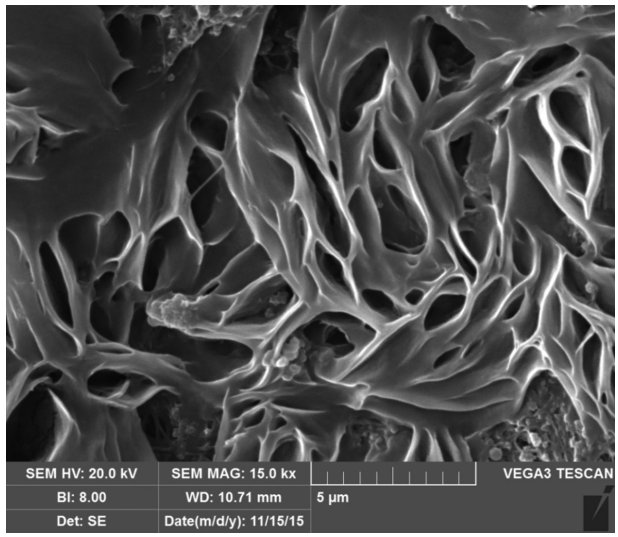


**Figure 1.** SEM micrograph of bacterial cellulose.

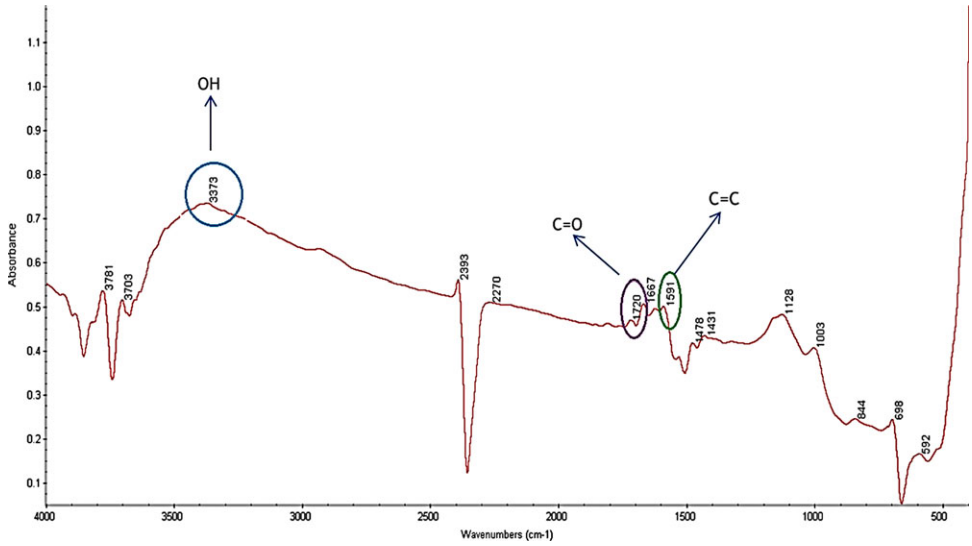


**Figure 2.** FTIR spectrum of bacterial cellulose.

As shown in Fig. 1 BC fibers are well-organized 3-D network structures and porous with interconnecting pores. The pore size varies in a certain range. The structures are nearly identical to those obtained by Wen et al. [25].

Figure 2 represents the FTIR spectra of the BC. The absorption band assigned to the hydroxyl and carboxyl groups is observed at 3373 and 1720 $cm^{-1}$, respectively. Furthermore, the peaks at 1591 $cm^{-1}$ is derived from aromatic skeletal vibrations (C=C). Also the carbonyl amide absorption band in 1667 $cm^{-1}$ may be the result of unwashed bacteria after treating with NaOH in BC purification process.

### 3.1.2 *Graphene oxide*

The results obtained from the preliminary analysis of GO are shown in Figs. 3–5. As shown in Fig. 3A synthesized GO was mostly single-layered with a topographic height of 2 nm according to AFM characterization (Fig. 3B). Raman spectroscopy is a nondestructive method that is widely used to obtain information from the carbon-based nanostructures. G and D are two main characteristic peaks in Raman spectroscopy. The peak G represents ordered organization of carbon atoms with $sp^2$ hybrid arrangement, while the peak D indicates the presence of incomplete sites on the graphene oxide (as well as functional groups bonded to the surface). As shown in Fig. 4 peak D and G appeared in the range of 1600 and 1300 $cm^{-1}$, respectively. Low intensity of peak D compared to peak G indicates that graphene has been generated with little defects. Graphene produced by Li and colleagues in 2013 have peak G in 1597 $cm^{-1}$ and peak D in 1358 $cm^{-1}$ [26]. In Ding and colleagues study, peak G and D was in the range of 1600 and 1340 $cm^{-1}$, respectively [27]. SEM and TEM micrographs in Figs. 5A and B confirmed AFM results as single-layered GO nanoparticles.

### 3.1.3 *Graphene oxide-silver nanohybrid*

The results obtained from the UV absorption analysis of GO-Ag nanohybrid are shown in Fig. 6. The absorption intensity of the

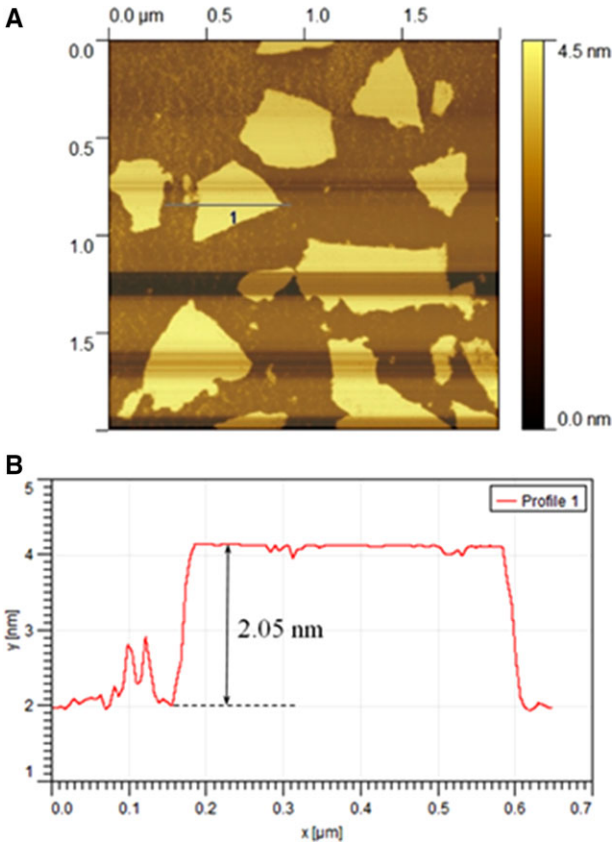


**Figure 3.** (A) AFM image and (B) height profile of GO.

peak at 420 nm increases gradually with an increase in Ag NPs concentration (Fig. 6B) that indicates higher levels of Ag NPs loaded on GO sheets, at optimized GO-Ag nanohybrid.

The FTIR spectra of GO and GO-Ag nanohybrid are shown in Fig. 7C. In GO, absorption peaks at 1050, 1200 and 1600 $cm^{-1}$ were attributed to the C–O stretching, C–O–C stretching and

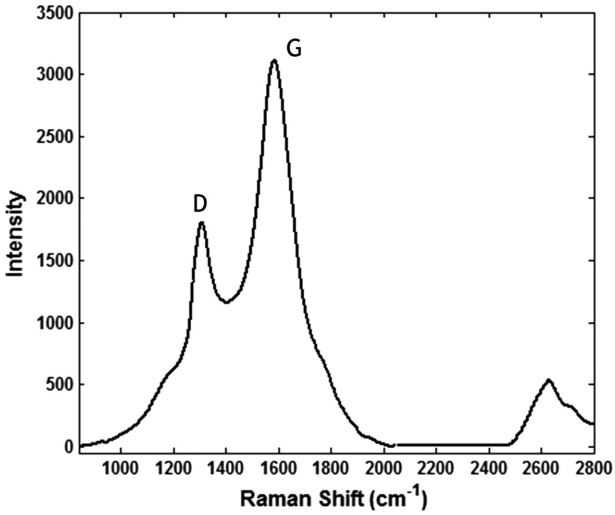


**Figure 4.** Raman spectra of GO.

C–O stretching, respectively. Oxygen related peaks demonstrated well oxidation of graphite by oxidation agents. In Fig. 7C (b), some peaks shifted and became lower ascribing to the reduction of GO. Resulted peaks are similar to data of Tian et al. that includes peaks in 1050 $cm^{-1}$ (C–O), 1218 $cm^{-1}$ (C–O–C) and 1725 $cm^{-1}$ (C=O) [28].

As shown in the TEM images (Figs. 7A and B), AgNPs uniformly distributed on the optimized GO-Ag surface in comparison to non-optimized GO-Ag.

### *3.1.4 Bacterial cellulose/graphene oxide-silver composite*

As shown in Figs. 8A and B nanoparticles impregnated in porous fibers of cellulose and made a smaller pore size and formed tangled and stronger structure that caused more mechanical resistance. Figs. 8C and D represents the X-ray diffraction (XRD) patterns of BC and BC/GO-Ag composite. As shown in Fig. 8C, BC shows a typical diffraction peak at around 39.58° and 26.64° which confirmed BC synthesis that with the combination of GO and BC the peaks become weak. Figure 5D around 17° corresponding to the GO indicates its uniform distribution on BC matrices.

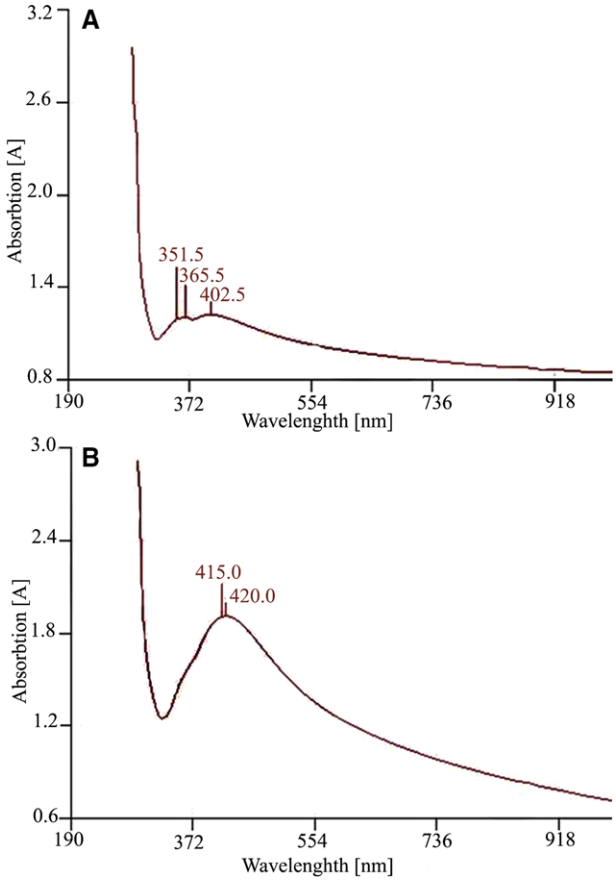


**Figure 6.** The absorption spectra of GO-Ag nanohybrid (A) non-optimized conditions (B) Optimized conditions.

## 3.2 Tensile strength and elongation tests

The tensile elongation values of the BC (as control) and reinforced BC with different weight percentage of GO-Ag nanohybrid (0.125, 0.25, 0.5 and 0.75) are shown in Fig. 9.

Tensile strength and Young's module of BC/GO-Ag composite with different weight percentage of GO-Ag nanohybrid are shown in Figs. 9F and G. Obviously, the addition of nanohybrid reinforced the ultimate tensile strength and increased the Young's Modulus. Remarkably, this improvement was achieved

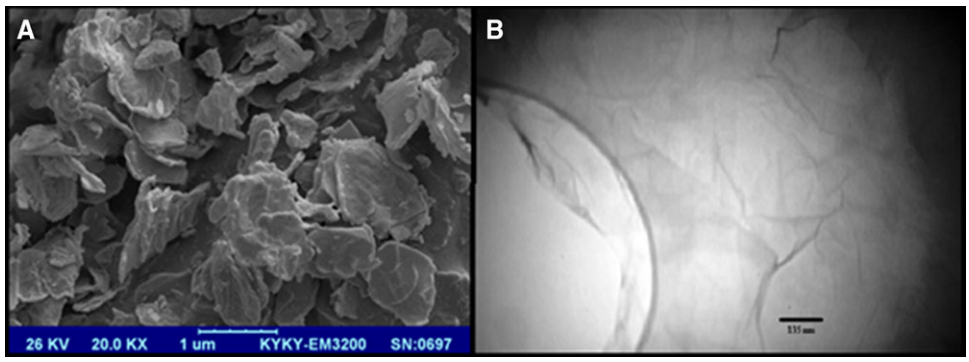


**Figure 5.** (A) TEM and (B) SEM micrograph of GO.

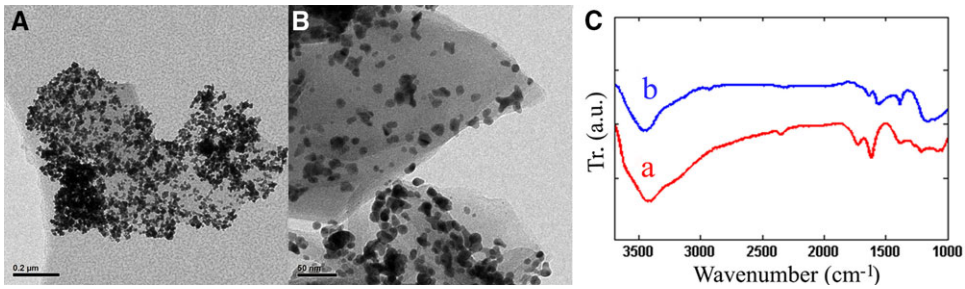


**Figure 7.** TEM images of GO-Ag nanohybrid (A) optimized conditions (B) non-optimized conditions and (C) FTIR spectrum of the GO (a) and GO-Ag nanohybrid (b).

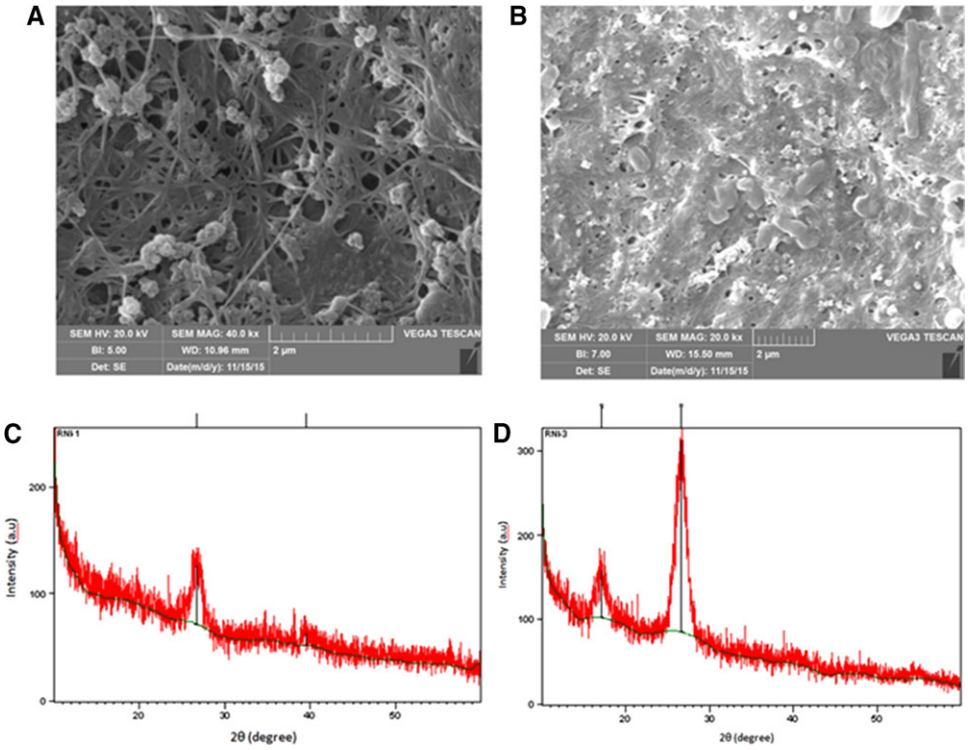


**Figure 8.** SEM images of (A) BC and (B) BC/GO-Ag nanocomposite and the XRD spectrum of the (C) BC and (D) BC/GO-Ag composite.

at a very low nanohybrid loading (0.1–0.2 wt.%). for instance, the incorporation of 0.2 wt.% nanohybrid increased the Young's Modulus 23% and TS 43% that is similar to the results of Tian et al. (2014) [28]. The increment of tensile strength should be attributed to the good coherence between the regenerated cellulose matrix and nanohybrid fillers, and the presence of strong interactions, which was confirmed by FTIR and XRD patterns.

### 3.3 Data analysis and evaluation of RSM model

The experiments were conducted based on the design matrix under the defined conditions. Responses obtained from the experimental runs are listed in Table 3. Thirteen experiments were conducted using the CCD method. Four experiments were repeated to estimate experimental errors.

The obtained responses were analyzed using response surface methodology. The GO suspension's pH and $\frac{[GO]}{[AgNO_3]}$ ratio are variable *A* and *B*, respectively. $R_1$ is the amount of silver loaded onto the GO sheets. Table 4 shows Analysis of variance.

According to the *p*-value ($p < 0.05$), variables *A* and $A^2$ are the important and effective factors. As a result, the final equation obtained for the $R_1$ response is as follows:

$$R_1 = 4.94 + 0.49A - 2.01A^2$$

The optimum conditions for $R_1$ response surface based on variable code was A = 0.04 and B = –0.82 that is equal to 7.48 and 0.068 for GO suspension's pH and $\frac{[GO]}{[AgNO_3]}$ ratio, respectively.

Figure 10 shows a 3-D Response surfaces for the CCD. As shown in Fig. 10, when the GO suspension's pH have a tendency to level 0 (pH = 7.4) and the $\frac{[GO]}{[AgNO_3]}$ ratio reduced to level −1 ($\frac{[GO]}{[AgNO_3]}$ =0.05), the amount of $R_1$ response increases, which is equivalent to increasing the amount of silver particles loaded on graphene sheets.

### 3.4 Antibacterial assay

The antibacterial properties of GO-Ag nanohybrid were investigated against *E. coli* and *S. aureus*. The MIC values for

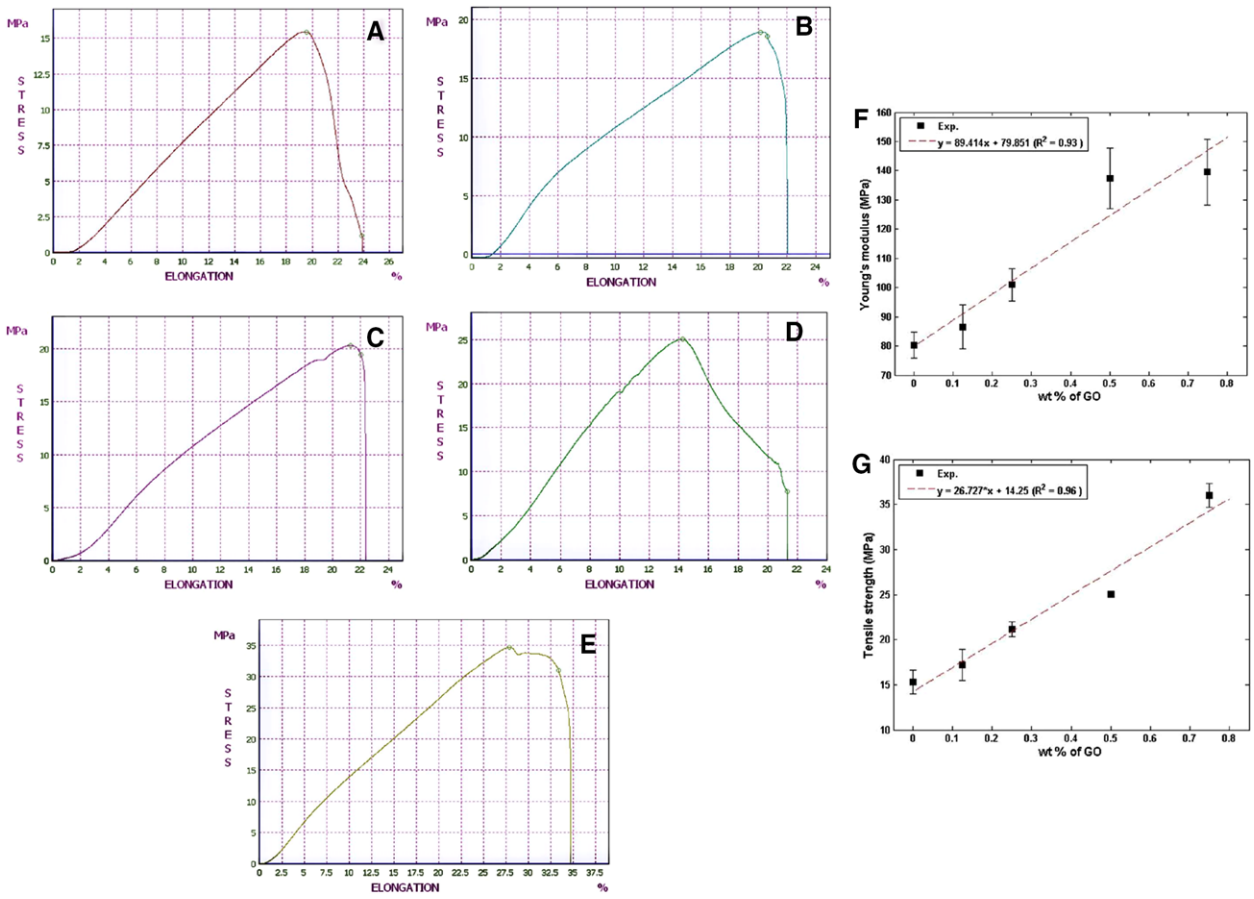


**Figure 9.** The tensile elongation of (A) BC, (B) BC with 0.125 wt.% nanohybrid, (C) BC with 0.25 wt.% of nanohybrid, (D) BC with 0.5 wt.% nanohybrid and (E) BC with 0.75 wt.% nanohybrid (F) Young's modulus and (G) Tensile strength of BC reinforced with different weight percentage.

**Table 3.** Experimental design matrix and results

| RUN | Experimental design | | |
|---|---|---|---|
| | pH | $\frac{[GO]}{[AgNO_3]}$ | Loaded silver |
| **1** | −1 | −1 | 3.42 |
| **2** | −1 | +1 | 4.52 |
| **3** | +1 | −1 | 1.90 |
| **4** | +1 | +1 | 3.25 |
| **5** | 0 | −1 | 2.00 |
| **6** | 0 | +1 | 2.51 |
| **7** | −1 | 0 | 3.92 |
| **8** | +1 | 0 | 4.31 |
| **9** | 0 | 0 | 5.27 |
| **10** | 0 | 0 | 5.07 |
| **11** | 0 | 0 | 4.97 |
| **12** | 0 | 0 | 5.17 |
| **13** | 0 | 0 | 5.00 |

**Table 4.** Analysis of variance for experimental responses at different factor levels

| Term | Sum of Sq. | Mean Sq. | *F* value | *p*-value |
|---|---|---|---|---|
| A | 1.46 | 1.46 | 2.28 | 0.105 |
| B | 0.96 | 0.96 | 1.5 | 0.2606 |
| AB | 0.016 | 0.016 | 0.024 | 0.8803 |
| A2 | 10.68 | 10.68 | 16.66 | 0.0047 |
| B2 | 0.031 | 0.031 | 0.049 | 0.8318 |

$R^2 = 0.8052$

these bacterial strains are shown in Table 5. The MIC of GO-Ag nanohybrid for *E. coli* and *S. aureus* were 0.01 and 0.17 mg/mL, respectively, which were lower than $AgNO_3$ suspension MIC values and in the case of gram-negative bacteria its bactericide effect was equal to the conventional antibiotic tetracycline. Taken together, the data from previous reports and the results presented here demonstrate that GO-Ag nanohybrid impart high bactericidal activities. Consequently, this will improve their potential applications in the medical field.

The antibacterial properties of BC/GO-Ag composite investigated by measuring OD of the bacteria cultured on pure BC and nanocomposite. *Escherichia coli* shows full growth on BC, while it was stopped at OD = 0.09 on BC/GO-Ag composite.

The antibacterial activity of Ag nanoparticles was investigated against Gram-negative bacterial strains *E. coli* and *P. aeruginosa*

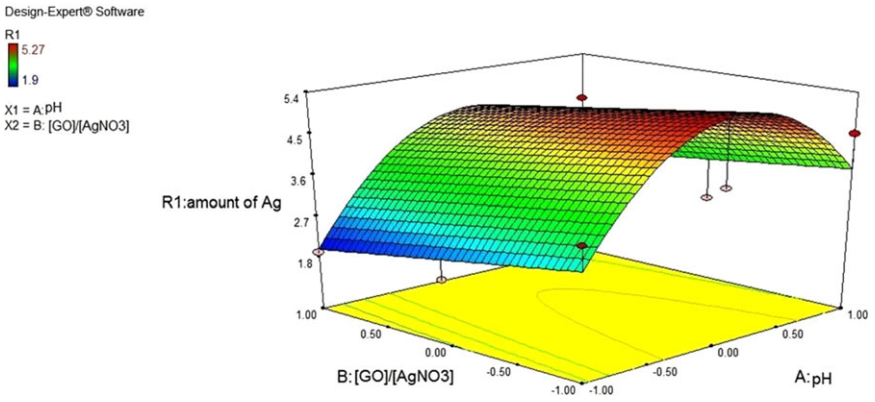


**Figure 10.** Effect of GO suspension's pH and $\frac{[GO]}{[AgNO_3]}$ on loaded silver on the surface of GO sheets.

**Table 5.** MIC values of the GO-Ag nanohybrid

| Bacteria | MIC | | |
|---|---|---|---|
| | GO-Ag nanohybrid | $AgNO_3$ suspansion | Tetracycline |
| *S. aureus* | 0.17 | 0.5 | 0.01 |
| *E. coli* | 0.01 | 0.09 | 0.01 |

in Das et al. study. It was observed that P. aeruginosa was more sensitive to the Ag nanoparticles which produced maximum growth inhibition zone. Additionally, the variation of Ag concentration during the synthesis of Ag nanoparticles affects bacterial growth [29]. In another study the antibacterial activity of freeze-dried silver nanoparticle-impregnated bacterial cellulose for was measured by the disc diffusion method. No inhibition zone was observed with the pure bacterial cellulose as control which shows the effect of Ag nanoparticles on bacteria [30]. Wu et al. compared the antibacterial effect of Ag nanoparticles/bacterial cellulose composite against *E. coli*, *S. aureus* and *P. aeruginosa*. The results showed that the antibacterial activity against *E. coli* and *P. aeruginosa* were lower than that against *S. aureus*. This observation is due to the difference in cell walls between Gram-positive and Gram-negative bacteria [10]. More studies about antibacterial activity of BC in combination with different materials is shown on Table 6.

## 4 Concluding remarks

The GO-Ag nanohybrid was synthesized. The effect of important parameters including GO suspension's pH and $\frac{[GO]}{[AgNO_3]}$ *ratio* was studied. The response surface methodology was employed to determine the most suitable processing conditions to attain optimized conditions. The GO-Ag nanohybrid impregnated to bacterial cellulose and its mechanical and antibacterial

**Table 6.** The result of antibacterial activity for different composites of BC

| Composite | Bacteria | Result | Reference | Year |
|---|---|---|---|---|
| Bacterial cellulose (BC) and montmorillonite (MMT) MMT, Na-MMT, Ca-MMT and Cu-MMT | *Escherichia coli and Staphylococcus aureus* | BC-Cu-MMT composites prepared with 2 and 4% MMT displayed clear zones of inhibition against *E. coli* and *S. aureus.* | [31] | 2013 |
| Silver nanoparticles into bacterial cellulose (BC) | *Escherichia coli* | Nearly 100% antibacterial activity | [32] | 2010 |
| Bacterial cellulose-Chitosan | *Escherichia coli* and *Staphylococcus aureus* | In the antibacterial test, the addition of chitosan in BC showed significant growth inhibition against *Escherichia coli* and *Staphylococcus aureus* | [33] | 2013 |
| BC-Ag nanocomposites | *Escherichia coli, Staphylococcus aureus, Bacillus subtilis* and *Candida albicans* | The experimental results showed BC-Ag nanocomposites have excellent anti-bacterial activities | [34] | 2015 |
| BC/sodium alginate (SA)- Silver sulfadiazine (AgSD) composites | *Escherichia coli, Staphylococcus aureus* and *Candida albicans* | The composite has excellent antibacterial activities and good biocompatibility | [35] | 2015 |
| SiO2 coated Cu nanoparticles (Cu@SiO2/BC) | *Staphylococcus aureus* and *Escherichia coli* | Excellent antibacterial activity | [36] | 2016 |
| ZnO-deposited BC composites | *Staphylococcus aureus* and *Escherichia coli* | Strong antibacterial activity without a photocatalytic reaction | [37] | 2016 |
| Bacterial cellulose-zinc oxide nanocomposites | *Escherichia coli, Pseudomonas aeruginosa, Staphylococcus aureus* and *Citrobacter freundii* | The composite exhibited 90, 87.4, 94.3 and 90.9% activity against *Escherichia coli, Pseudomonas aeruginosa, Staphylococcus aureus* and *Citrobacter freundii*, respectively | [38] | 2017 |

properties investigated. The presence of GO-Ag nanohybrid increased the mechanical strength and antibacterial activity of bacterial cellulose. Taken together, the present study indicates that BC impregnated with GO-Ag nanohybrid is a potential wound dressing material. However, more work on clinical wounds of smaller and larger animals will need to be done before its application on to humans.

## Practical application

The present work describes the synthesis processes and characterization of a potential wound dressing material based on graphene oxide/silver nanocomposite-coated bacterial cellulose. The prepared nanocomposite was characterized for their morphological properties, mechanical properties and antibacterial activity. It shows very good antibacterial properties and mechanical strength that made it a good choice for medical applications and future use.

*The authors have declared no conflict of interest.*

## 5 References

[1] Sulaeva, I., Henniges, U., Rosenau, T., Potthast, A., Bacterial cellulose as a material for wound treatment: properties and modifications: a review. *Biotechnol. Adv.* 2015, *33*, 1547–1571.
[2] Shah, N., Ul-Islam, M., Khattak W. A., Park J. K., Overview of bacterial cellulose composites: a multipurpose advanced material. *Carbohydr. Polym.* 2013, *98*, 1585–1598.
[3] Zhu, W., Li, W., He, Y., Duan, T., In-situ biopreparation of biocompatible bacterial cellulose/graphene oxide composites pellets. *Appl. Surf. Sci.* 2015, *338*, 22–26.
[4] Moghimi S. M., Farhangrazi Z. S., Just so stories: the random acts of anti-cancer nanomedicine performance. *Nanomedicine* 2014, *10*, 1661–1666.
[5] Beyth, N., Houri-Haddad, Y., Domb, A., Khan, W. et al., Alternative antimicrobial approach: nano-antimicrobial materials. *Evid. Based Complementary Altern Med.* 2015, *2015*, 246012.
[6] Ravishankar Rai, V., Jamuna Bai, A., Nanoparticles and their potential application as antimicrobials. *Formatex* 2011, 197–209.
[7] Galdiero, S., Falanga, A., Vitiello, M., Cantisani, M. et al., Silver nanoparticles as potential antiviral agents. *Molecules* 2011, *16*, 8894–8918.
[8] Maneerung, T., Tokura, S., Rujiravanit, R., Impregnation of silver nanoparticles into bacterial cellulose for antimicrobial wound dressing. *Carbohydr. Polym.* 2008, *72*, 43–51.
[9] de Santa Maria, L.C., Santos, A. L. C., Oliveira, P. C., Barud, H. S. et al., Synthesis and characterization of silver nanoparticles impregnated into bacterial cellulose. *Mater. Lett.* 2009, *63*, 797–799.
[10] Wu, J., Zheng, Y., Song, W., Luan, J. et al., In situ synthesis of silver-nanoparticles/bacterial cellulose composites for slow-released antimicrobial wound dressing. *Carbohydr. Polym.* 2014, *102*, 762–771.
[11] Katepetch, C., Rujiravanit, R., Tamura, H., Formation of nanocrystalline ZnO particles into bacterial cellulose pellicle by ultrasonic-assisted in situ synthesis. *Cellulose* 2013, *20*, 1275–1292.
[12] Khan, S., Ul-Islam, M., Khattak W. A., Ullah M. W. et al., Bacterial cellulose-titanium dioxide nanocomposites: nanostructural characteristics, antibacterial mechanism, and biocompatibility. *Cellulose* 2015, *22*, 565–579.
[13] Shao, W., Liu, H., Liu, X., Wang, S. et al., Antibacterial performances and biocompatibility of bacterial cellulose/graphene oxide composites. *RSC Adv.* 2015, *5*, 4795–4803.
[14] Ma, J., Zhang, J., Xiong, Z., Yong, Y. et al., Preparation, characterization and antibacterial properties of silver-modified graphene oxide. *J. Mater. Chem.* 2011, *21*, 3350.
[15] Hur, J., Shin, J., Yoo, J., Seo Y. S., Competitive adsorption of metals onto magnetic graphene oxide: comparison with other carbonaceous adsorbents. *Sci. World J.* 2015, *2015*, 1–11.
[16] Puértolas, B., Mayoral, Á., Arenal, R., Solsona, B. et al., High-temperature stable gold nanoparticle catalysts for application under severe conditions: the role of TiO2 nanodomains in structure and activity. *ACS Catal.* 2015, *5*, 1078–1086.
[17] Das, M. R., Sarma, R. K., Borah, S. C., Kumari, R. et al., The synthesis of citrate-modified silver nanoparticles in an aqueous suspension of graphene oxide nanosheets and their antibacterial activity. *Colloids Surf. B Biointerfaces* 2013, *105*, 128–136.
[18] De Faria, A. F., Martinez, D. S. T., Meira, S. M. M., de Moraes, A. C. M. et al., Anti-adhesion and antibacterial activity of silver nanoparticles supported on graphene oxide sheets. *Colloids Surf. B Biointerfaces* 2014, *113*, 115–124.
[19] Yun, H., Kim, J. D., Choi, H. C., Lee, C. W., Antibacterial activity of CNT-Ag and GO-Ag nanocomposites against gram-negative and gram-positive bacteria. *Bull. Korean Chem. Soc.* 2013, *34*, 3261–3264.
[20] Santos, S. M., Carbajo, J. M., Quintana, E., Ibarra, D. et al., Characterization of purified bacterial cellulose focused on its use on paper restoration. *Carbohydr. Polym.* 2015, *116*, 173–181.
[21] Santosh, S., Bhanureka, Graphene based piezo resistive sensor fabrication and its characterization, in: *Second Internationa Conference on Recent Advances in Science & Engineering-2015*, 2015.
[22] Mehl, H., Oliveira, M. M., Zarbin, A. J. G., Thin and transparent films of graphene/silver nanoparticles obtained at liquid-liquid interfaces: preparation, characterization and application as SERS substrates. *J. Colloid Interface Sci.* 2015, *438*, 29–38.
[23] Jo, D. H., Lee, C. H., Jung, H., Jeon, S. et al., Effect of amine surface density on CO2 adsorption behaviors of amine-functionalized polystyrene. *Bull. Chem. Soc. Japan* 2015, *88*, 1317–1322.
[24] ASTM, D 882: standard test method for tensile properties of thin plastic sheeting. *Astm* 2002, *14*, 1–10.
[25] Wen, X., Zheng, Y., Wu, J., Yue, L. et al., In vitro and in vivo investigation of bacterial cellulose dressing containing uniform silver sulfadiazine nanoparticles for burn wound healing. *Prog. Natural Sci. Mater. Int.* 2015, *25*, 197–203.
[26] Li, C., Wang, X., Chen, F., Zhang, C. et al., The antifungal activity of graphene oxide-silver nanocomposites. *Biomaterials* 2013, *34*, 3882–3890.

[27] Ding, G., Xie, S., Liu, Y., Wang, L. et al., Graphene oxide-silver nanocomposite as SERS substrate for dye detection: effects of silver loading amount and composite dosage. *Appl. Surf. Sci.* 2015, *345*, 310–318.

[28] Tian, M., Qu, L., Zhang, X., Zhang, K. et al., Enhanced mechanical and thermal properties of regenerated cellulose/graphene composite fibers. *Carbohydr. Polym.* 2014, *111*, 456–462.

[29] Das, M. R., Sarma, R. K., Saikia, R., Kale, V. S. et al., Synthesis of silver nanoparticles in an aqueous suspension of graphene oxide sheets and its antimicrobial activity. *Colloids Surf. B Biointerfaces* 2011, *83*, 16–22.

[30] Maneerung, T., Tokura, S., Rujiravanit, R., Impregnation of silver nanoparticles into bacterial cellulose for antimicrobial wound dressing. *Carbohydr. Polym.* 2008, *72*, 43–51.

[31] Ul-Islam, M., Khan, T., Khattak, W. A., Park, J. K., Bacterial cellulose-MMTs nanoreinforced composite films: novel wound dressing material with antibacterial properties. *Cellulose* 2013, *20*, 589–596.

[32] Maria, L., Santos, A. L., Oliveira, P. C., Valle, A. S. et al., Preparation and antibacterial activity of silver nanoparticles impregnated in bacterial cellulose. *Polimeros.* 2010, *20*, 72–77.

[33] Lin, W.-C., Lien, C.-C., Yeh, H.-J., Yu, C.-M. et al., Bacterial cellulose and bacterial cellulose–chitosan membranes for wound dressing applications. *Carbohydr. Polym.* 2013, *94*, 603–611.

[34] Shao, W., Liu, H., Liu, X., Sun, H. et al., pH-responsive release behavior and anti-bacterial activity of bacterial cellulose-silver nanocomposites. *Int. J. Biol. Macromol.* 2015, *76*, 209–217.

[35] Shao, W., Liu, H., Liu, X., Wang, S. et al., Development of silver sulfadiazine loaded bacterial cellulose/sodium alginate composite films with enhanced antibacterial property. *Carbohydr. Polym.* 2015, *132*, 351–358.

[36] Ma, B., Huang, Y., Zhu, C., Chen, C. et al., Novel Cu@SiO2/bacterial cellulose nanofibers: Preparation and excellent performance in antibacterial activity. *Mater. Sci. Eng. C Mater. Biol. Appl.* 2016, *62*, 656–661.

[37] Janpetch, N., Saito, N., Rujiravanit, R., Fabrication of bacterial cellulose-ZnO composite via solution plasma process for antibacterial applications. *Carbohydr. Polym.* 2016, *148*, 335–344.

[38] Khalid, A., Khan, R., Ul-Islam, M., Khan, T. et al., Bacterial cellulose-zinc oxide nanocomposites as a novel dressing system for burn wounds. *Carbohydr. Polym.* 2017, *164*, 214–221.